Available online at www.sciencedirect.com
ScienceDirect
Icarus ••• (••••) •••–•••
ICARUS
www.elsevier.com/locate/icarus

The effects of ablation on the cross section of planetary envelopes at capturing planetesimals

Omar G. Benvenuto [a,b,1,*], Adrián Brunini [a,b,2]

[a] *Facultad de Ciencias Astronómicas y Geofísicas, Universidad Nacional de La Plata, Paseo del Bosque S/N, 1900 La Plata, Argentina*
[b] *Instituto de Astrofísica de La Plata (IALP), Paseo del Bosque S/N, 1900 La Plata, Argentina*

Received 8 June 2007; revised 13 February 2008

Abstract

We explore the cross section of giant planet envelopes at capturing planetesimals of different sizes. For this purpose we employ two sets of realistic planetary envelope models (computed assuming for the protoplanetary nebula masses of 10 and 5 times the mass of the minimum mass solar nebula), account for drag and ablation effects and study the trajectories along which planetesimals move. The core accretion of these models has been computed in the oligarchic growth regime [Fortier, A., Benvenuto, O.G., Brunini, A., 2007. Astron. Astrophys. 473, 311–322], which has also been considered for the velocities of the incoming planetesimals. This regime predicts velocities larger that those used in previous studies of this problem. As the rate of ablation is dependent on the third power of velocity, ablation is more important in the oligarchic growth regime. We compute energy and mass deposition, fractional ablated masses and the total cross section of planets for a wide range of values of the critical parameter of ablation. In computing the total cross section of the planet we have included the contributions due to mass deposited by planetesimals moving along unbound orbits. Our results indicate that, for the case of small planetary cores and low velocities for the incoming planetesimals, ablation has a negligible impact on the capture cross section in agreement with the results presented in Inaba and Ikoma [Inaba, S., Ikoma, M., 2003. Astron. Astrophys. 410, 711–723]. However for the case of larger cores and high velocities of the incoming planetesimals as predicted by the oligarchic growth regime, we find that ablation is important in determining the planetary cross section, being several times larger than the value corresponding ignoring ablation. This is so regardless of the size of the incoming planetesimals.

Keywords: Accretion; Planetary formation; Planetesimals

1. Introduction

The core instability (see, e.g., Mizuno, 1980; Bodenheimer and Pollack, 1986; Pollack et al., 1996) is at present the most widely accepted mechanism to account for giant planet formation. In this model, a planetary embryo first grows by the accretion of solid material during pairwise collisions of planetesimals. As the core grows, it binds an increasing amount of the surrounding primordial gas. If the core reaches some Earth's masses while the gas is still present in the nebula, the tendency of the envelope to undergo a gravitational collapse cannot longer be equilibrated by the pressure gradient within the envelope, and a runaway gas accretion begins. This process leads to the formation of a giant planet.

In a protoplanetary disk, the first mode of solid accretion is runaway growth, where the largest bodies grow much faster than the smaller ones. In this regime, self-interactions dominate the dynamical evolution of the planetesimals disk, the relative velocities are low, and the gravitational cross section of the big planetesimals is the largest one (Greenberg et al., 1978; Kokubo and Ida, 1996). However, at later times, the largest objects become massive enough such that their dynamical influence dominates the relative velocities of the surrounding planetesimals. Then, the growth process switches to a slower

* Corresponding author at: Facultad de Ciencias Astronómicas y Geofísicas, Universidad Nacional de La Plata, Paseo del Bosque S/N, 1900 La Plata, Argentina.
E-mail address: obenvenu@fcaglp.unlp.edu.ar (O.G. Benvenuto).
[1] Member of the Carrera del Investigador Científico, Comisión de Investigaciones Científicas de la Provincia de Buenos Aires (CIC).
[2] Member of the Carrera del Investigador Científico, Consejo Nacional de Investigaciones Científicas y Técnicas (CONICET).

0019-1035/$ – see front matter © 2008 Published by Elsevier Inc.
doi:10.1016/j.icarus.2008.02.012

regime. The embryos stir the relative velocities of the planetesimals whose accretion is almost interrupted. So, the embryos are the only bodies that grow substantially at this stage. For this reason, this mode of accretion was called "oligarchic growth" (Ida and Makino, 1993; Kokubo and Ida, 1998). The transition from runaway to oligarchic growth occurs when the protoplanets are of lunar size. Therefore, since very early times, the relevant regime for modeling the accretion of solid cores of giant planets is oligarchic growth.

Nevertheless, for relative velocities, Pollack et al. (1996) adopted the results of calculations by Greenzweig and Lissauer (1990, 1992). In this model, the planetesimals' inclination is controlled by their mutual gravitational scatterings, and their eccentricities are determined by a combination of the scatterings and gravitational interactions with the protoplanet at distances comparable to its Hill sphere radius. The corresponding expressions are

$$\begin{aligned}\langle i^2\rangle^{1/2} &= \frac{1}{\sqrt{3}}\frac{v_{\rm esc}}{v_K},\\ \langle e^2\rangle^{1/2} &= \max\{2\langle i^2\rangle^{1/2}, 2h_r\},\end{aligned} \tag{1}$$

where $v_{\rm esc}$ is the escape velocity from the surface of a planetesimal, v_K is the circular Keplerian orbital velocity at the protoplanet distance from the central star and $h_r = (M_P/3M_*)^{1/3}$ is the reduced Hill's radius of the protoplanet of mass M_P. M_* is the mass of the central star of the system.

On another hand, in oligarchic grow models, planetesimals attain an equilibrium *r.m.s* eccentricity when the perturbations due to protoplanets are balanced by dissipation due to gas drag. Following Ida and Makino (1993) (see also Thommes et al., 2003), the equilibrium value for planetesimals of mass m_p is given by

$$\begin{aligned}\langle e^2\rangle^{1/2} &= 0.04\left(\frac{\rho_{\rm gas}}{1.4\times10^{-9}\ {\rm g\,cm^{-3}}}\right)^{-1/5}\\ &\quad\times\left(\frac{m_p}{10^{-9}M_\oplus}\right)^{1/15}\left(\frac{r_*}{1\ {\rm AU}}\right)^{(\alpha-1)/5}\left(\frac{M_P}{1M_\oplus}\right)^{1/3},\\ \langle i^2\rangle^{1/2} &= \langle e^2\rangle^{1/2}/2,\end{aligned} \tag{2}$$

where we have assumed that the nebular gas density $\rho_{\rm gas}$ has a profile of the form $\rho_{\rm gas}\propto r_*^{-\alpha}$ where r_* is the distance from the central star of the system.

Fig. 1 shows the ratio between the prescriptions of the planetesimal velocity given by Eqs. (1) and (2), as a function of the planet's mass, for planetesimals of different sizes. Throughout this paper the planet is placed at a distance of 5 AU from the Sun. The gaseous nebular density $\rho_{\rm gas}$ is the one prescribed by the minimum mass solar nebula (hereafter MMSN) model of Hayashi (1981):

$$\rho_{\rm gas} = 1.4\times10^{-9}\left(\frac{r_*}{1\ {\rm AU}}\right)^{-11/4}\ {\rm g\,cm^{-3}}. \tag{3}$$

It is evident that planetesimal velocities predicted in the oligarchic growth model are larger than those given by Eq. (1) by a non-negligible factor. Therefore, remarkably, several models of giant planet formation in the frame of the core instability,

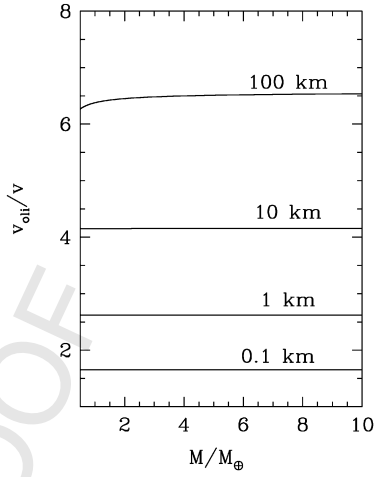

Fig. 1. The ratio of the velocity of planetesimals in the oligarchic growth regime and the velocities given by Greenzweig and Lissauer (1990, 1992) as a function of the mass of the planet. Notice that velocities in the oligarchic growth regime are much higher. This has a direct impact on the ablation rate of planetesimals because it depends with velocity as v^3.

have used planetesimal velocities slower than the equilibrium velocities attained in the oligarchic growth regime. Some researchers have considered such a regime. For example, Ikoma et al. (2000) have studied the formation of gaseous envelopes assuming an initial runaway and subsequent oligarchic regime for the core growth up to little after the onset of the runaway gas accretion. They employed a prescription for core accretion which is only function of the planetesimals surface density, the core mass of the protoplanet and the distance from the central star. So, they did not considered the enhancement of the capture cross section due to the structure of the planetary envelope. Also, more recently, Inaba et al. (2003) have calculated formation of gas giant planets based on the standard core accretion model including effects due to fragmentation, the presence of a planetary envelope and the perturbations between the planetary embryos and the remaining planetesimals which, in turn, enhance the relevance of fragmentation. They found embryos massive enough to start a fast gas accretion phase. To our knowledge, to date, the only work that considered the whole process of planetary formation in the frame of the oligarchic growth regime, getting Jupiter mass objects, is that of Fortier et al. (2007), although in this work fragmentation and migration of planetesimals have not been included.

Low velocities have impact in the accretion rates, but the relative velocity plays also a crucial role in the interaction of the planetesimals with the planetary envelope during the accretion process, which is an important piece of the model. Podolak et al. (1988), Brunini and Melita (2002), Inaba and Ikoma (2003), Alibert et al. (2005), and Fortier et al. (2007) have shown that planetesimals interact with the envelope gas. In particular, gas drag affects planetesimal velocities, enhancing the effective cross section of the planet relative to the gravitational cross section by a large factor. Therefore, this effect is important in shortening the formation time scale.

Planetesimals are also ablated by the interaction with the gas of the envelope. Recently, it has been considered that the effects

Please cite this article in press as: O.G. Benvenuto, A. Brunini, The effects of ablation on the cross section of planetary envelopes at capturing planetesimals, Icarus (2008), doi:10.1016/j.icarus.2008.02.012

due to ablation are negligible in determining the total cross section of a planet for capturing planetesimals (Inaba and Ikoma, 2003). Here, we shall show below that effects due to ablation in the oligarchic growth regime are important, and in fact may increase the planetary cross section several times. This is so especially for the case of planetary cores larger than those considered by Inaba and Ikoma (2003). This is the main purpose of the present paper. In doing so, we shall perform a systematic exploration of the effects of drag and ablation for two sets of planetary envelope models (see below, Section 2 for details) and a wide range of parameters describing ablation.

The paper is organized as follows: in Section 2 we describe the models of planetary envelopes employed for this study. Section 3 is devoted to describe the equations of motion of the planetesimals and to give details of the numerical procedures we have employed. In Section 4 we present the numerical results we have found and finally, in Section 5 we present a discussion and some concluding remarks on the relevance of the results presented in this paper.

2. Planetary envelope models

In order to perform a detailed calculation of the effects of drag and ablation on the cross section of planets at capturing planetesimals we shall employ two different sets of models, each of them composed by eight planetary envelopes taken from two of our own evolutionary calculations. Both sets of models have been computed employing the scheme presented in Benvenuto and Brunini (2005) updated by Fortier et al. (2007) in order to consider the core accretion process as dominated by the oligarchic growth regime. To our knowledge, the planetary models presented in Fortier et al. (2007) are the only ones constructed in the frame of such regime.

The set of models selected for the present study have been grown from a $10^{-6} M_\oplus$ embryo at a fixed orbital distance $a = 5.2$ AU. Set I (II) corresponds to the formation of a giant planet immersed in a protoplanetary nebula with a mass in gas and dust corresponding to 10 (5) times that of the MMSN.

We should remark that in the computation of the core accretion process of the planetary models presented in Fortier et al. (2007), the velocity regime of the planetesimals is the same we shall employ as initial condition for the velocity of the incoming planetesimals (see Section 1). So, this study is consistent in this aspect. However, in constructing these models planetary models we have *not* considered the effects due to ablation (see below, Section 4) in the calculation of the capture cross section. The construction of planetary models considering the treatment of the capture cross section presented below, beyond the scope of this paper, is underway and will be reported elsewhere.

The main criterion in selecting these sets of models, and the specific models in each of them has been to include density profiles representative of all stages of planetary formation. We do so with the aim of getting a global view of the relevance of the effects of drag and ablation in computing the effective cross section of planetary envelopes in the oligarchic growth regime.

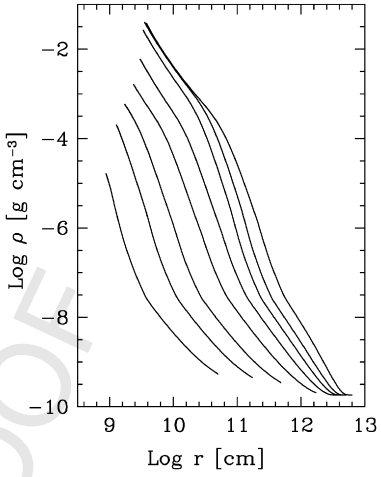

Fig. 2. The density profiles corresponding to the set I of the planetary envelopes considered in this paper, whose main characteristics are given in Table 1. From left to right curves correspond to models labeled as A, ..., H.

Table 1
Some characteristics of the planetary envelope models considered in this paper

Model	Age [Myr]	$\log R_P$ [cm]	$M_{\rm env}$ [$M_\oplus$]	$M_{\rm core}$ [$M_\oplus$]	$\log \rho_b$ [g cm^{-3}]	$\log T_b$ [K]
A	0.6496	10.6201	0.00007	1.44077	−4.77518	3.45545
B	0.8652	11.1479	0.00254	4.46024	−3.69047	3.74044
C	1.0021	11.5966	0.04250	10.8935	−3.22932	4.03685
D	1.1401	12.1529	0.96390	28.2889	−2.78772	4.31043
E	1.2801	12.4994	8.03730	57.2729	−2.22007	4.46537
F	1.4698	12.5758	30.1687	80.5983	−1.57319	4.56332
G	1.6331	12.6377	75.8051	93.9489	−1.39501	4.60793
H	1.7562	12.7191	185.419	112.597	−1.41819	4.64521
A*	3.3180	10.4493	0.00013	0.74315	−5.30258	3.29276
B*	4.8253	10.8137	0.00219	1.76425	−3.82622	3.48615
C*	6.9674	11.2009	0.06172	4.90754	−2.82559	3.79371
D*	8.8800	11.6433	0.11256	11.7846	−2.27213	4.07910
E*	10.5396	11.9525	0.83010	19.8781	−1.84727	4.25673
F*	12.8504	12.2457	6.65948	26.8801	−1.31455	4.36944
G*	16.1726	12.5456	52.4138	37.4077	−1.17508	4.48127
H*	16.7627	12.7179	246.643	48.7900	−1.60661	4.52071

From left to right, the columns give the label of the model, its age, the logarithm of the planetary radius, the mass of the envelope, the mass of the core, the logarithm of the density and the logarithm of the temperature, both at the bottom of the envelope, respectively.

The density profiles for the set of models I are shown in Fig. 2 (the profiles corresponding to the set of models II are qualitatively similar) while the main characteristics of both sets of selected models are presented in Table 1. Throughout this paper we shall refer the models with letters A, ..., H and A*, ..., H* for sets I and II respectively.

As consequence of the regime assumed for the growth of the planetary core, models are very different to those previously computed by other authors (e.g., Pollack et al., 1996; Alibert et al., 2005). While a detailed discussion of the differences of our models as compared to those computed by other authors has been presented in Fortier et al. (2007), some remarks are in order here.

In their calculations, Pollack et al. (1996) found three main stages of giant planet formation. This is well described in their

Please cite this article in press as: O.G. Benvenuto, A. Brunini, The effects of ablation on the cross section of planetary envelopes at capturing planetesimals, Icarus (2008), doi:10.1016/j.icarus.2008.02.012

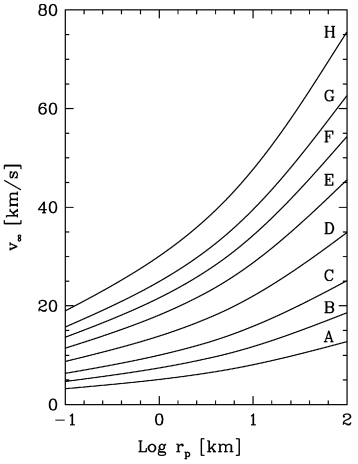

Fig. 3. The velocity of planetesimals at entering the planetary envelopes corresponding to the set of models I as a function of the planetesimal sizes.

Fig. 1 (particularly Fig. 1b) which corresponds to the formation of a Jupiter-like object located in an environment with a solids surface density of 10 g cm^{-2}: The first stage is a runaway accretion of solids (≈0.5 Myr), followed by a period of ≈7.5 Myr in which the accretion rate is substantially lower, and finally the third stage is the runaway gas accretion. Clearly, the timescale of the whole process is dominated by the second stage. In Fortier et al. (2007), we computed some specific models to allow for a quantitative comparison with the above discussed model of Pollack et al. (1996), in particular, those we presented in Fig. 3 of our previous paper. While Pollack et al. (1996) find that the rate of accretion of solids is equal to that of gas at ≈0.75 Myr, we find it to be the case after 16 Myr, meanwhile the second stage of low rate for the accretion of solids is completely absent in our calculations. Pollack et al. (1996) find the onset of the runaway gas accretion after 8 Myr when the core mass is $\approx 20 M_\oplus$ while we find it at an age of 20 Myr with a core mass of $42 M_\oplus$.

One may be worried because the timescale for the whole process of planetary formation is apparently too long as compared to the timescale for the dissipation of the gaseous protoplanetary nebula (Hollenbach et al., 2000) and/or because of the mass of the core as compared to the currently estimated mass of Jupiter's core (Guillot, 2005). In this sense, it is important to remind the reader the approximations made in Pollack et al. (1996) as well as in Fortier et al. (2007). In both sets of computations it was considered that the planet grows alone, that all planetesimals have one fixed size, and there is no migration. The relaxation of any of these approximations may change the present description of planetary formation, even qualitatively. Obviously, it warrants a detailed investigation but this is beyond the scope of the present work. Thus, the sets models we shall employ in this paper should be considered as plausible in the frame of the oligarchic growth regime. Because of the differences in the masses of the protoplanetary nebulae in which planetary models have been grown (5 and 10 MMSN), the results to be described below should be useful to guide our expectations when considering more detailed models of the whole process of planetary formation.

3. Handling planetesimals

3.1. Equations of motion

In computing planetesimal trajectories, we shall consider the description adopted by Inaba and Ikoma (2003). The equation of motion of planetesimals is given by the contributions due to gravitation and drag force

$$m_p \frac{\mathrm{d}\vec{v}}{\mathrm{d}t} = -\frac{G M_P(r) m_p}{r^3}\vec{r} - D\pi r_p^2 \rho(r) v \vec{v}. \quad (4)$$

Here G is the gravitational constant, $m_p(r_p)$ is the mass (radius) of the planetesimal, $\vec{v}$ its velocity, $M_P(r)$ is the mass of the planet interior to r (including the core), $\rho(r)$ is the density of the gaseous envelope at r, and D is the drag coefficient. We shall neglect the effects due to the presence of the central star of the system. Ablation is included by means of

$$\frac{\mathrm{d}m_p}{\mathrm{d}t} = -\sigma_{\mathrm{ab}} D\pi r_p^2 \rho(r) v^3, \quad (5)$$

where σ_{ab} is the ablation coefficient. We shall consider planetesimals as spherical with a constant density $\rho_p = 1.5$ g cm^{-3}.

In computing the trajectory of the planetesimals we shall integrate Eqs. (4)–(5) by means of an adaptive Runge–Kutta routine (Press et al., 1992). Regarding the quantities dependent on the structure of the planetary envelope, we performed a linear interpolation in the logarithm of the density and the total mass. Thus, we shall include the contribution of the mass of the envelope in the simulations. The initial conditions for the trajectories is that the velocity of the planetesimals v_∞ is the one corresponding to the oligarchic growth regime (given by Eqs. (2)) and its position is at the planetary surface.[3] The corresponding values for the set of models I are depicted in Fig. 3. For the case of the set of models II, the values are similar.

Here we shall consider values of the impact parameter a from the planetary radius up to $10^{-3} R_P$ with relative steps of 5×10^{-3}. It is worth noticing that the equilibrium value for the planetesimal velocity is a good approximation in this case, even for very small planetesimals, because we are working with massive embryos (Thommes et al., 2003; Chambers, 2006).

3.2. On the coefficient of ablation

A key ingredient in this study is the value of the ablation coefficient σ_{ab}. A useful discussion of this problem is presented in Alibert et al. (2005) and references therein.

For the case of small meteorites, $\sigma_{\mathrm{ab}} = 0.1$ s^2 km^{-2} is adequate to account for available observational data. However, for the case of large incoming planetesimals like those we are interested in here, such a value is too large and values of σ_{ab} of two or even three orders of magnitude lower are in order. This has been found by studying the collision of Comet Shoemaker–Levy 9 onto Jupiter. As we are interested in the case of planetes-

[3] As usual, we considered the planetary surface located at a radius given by the minimum between the Hill radius $R_H = a h_r$ and the accretion radius $R_A = G M_P / c_s^2$. Here, M_P the planetary mass, and c_s the local velocity of sound.

Please cite this article in press as: O.G. Benvenuto, A. Brunini, The effects of ablation on the cross section of planetary envelopes at capturing planetesimals, Icarus (2008), doi:10.1016/j.icarus.2008.02.012

imals of several sizes, ideally we would need $\sigma_{ab}(r_p)$ which is, at present, very uncertain.

Unfortunately, the results we shall find are strongly dependent on σ_{ab}. Thus, all the results will be directly affected by the above mentioned uncertainty. Because of this reason, we shall simply explore a wide range of values of σ_{ab} that (hopefully) will include the actual values of this critical parameter. With such a procedure we shall be able to evaluate the necessity of a more detailed treatment of ablation than the one employed in the present paper at calculating capture cross sections. In particular, we shall consider $\sigma_{ab} = 10^{-1}$, 10^{-2}, 10^{-3}, 10^{-4}, and 10^{-5} s^2 km^{-2}.

4. Numerical results

4.1. The trajectories of planetesimals

There are three kinds of trajectories: those that remain open, with a large impact parameter a (comparable to the planetary radius) for which drag and ablation are not able to dissipate enough energy and the planetesimals leave the planet (class A). Other trajectories, with intermediate impact parameter will become bounded due to drag and ablation (class B). For a given planetesimal size, there exists a critical impact parameter a_{crit} separating these two behaviors. Finally, there are trajectories starting with a much smaller impact parameter that collide directly onto the core (class C), see Fig. 4.

For unbounded orbits we shall compute them up to the moment at which the planetesimal leaves the planet but we shall *include* the effects of energy and material deposition in the envelope layers along the planetesimal trajectory. For trajectories that become bounded we shall compute them up to the moment at which the mass of the planetesimal becomes $\leqslant 10^{-6}$ of the original mass or when it collides the core.

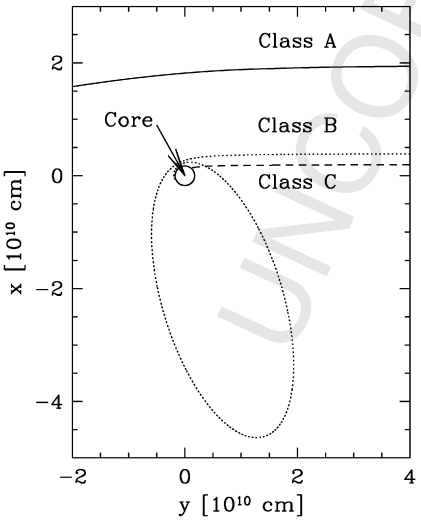

Fig. 4. The three kinds of orbits for incoming planetesimals. Full line depicts an open orbit that leaves the planet, dotted line represents an orbit that spirals in and is captured by drag and ablation and finally, dashed line shows the case of a direct collision onto the core. In this case we employed the envelope C, for which the planetary surface is far outside the adopted scale.

4.2. Energy deposition on protoplanetary layers

Now, let us compute the energy deposition per units of time and mass $\varepsilon(r_p)$ due to planetesimals of radius r_p[4]. Let us define $\Phi(M_r, a, r_p)$ as the energy deposited per gram on a layer between M_r and $M_r + \mathrm{d}M_r$ incoming with an impact parameter a. In order to add contributions due to different impact parameters, we have to compute the number $\mathrm{d}N$ of incoming planetesimals per second between a and $a + \mathrm{d}a$, which is

$$\frac{\mathrm{d}N}{\mathrm{d}t} = 2\pi a n(r_p) v_\infty(r_p)\,\mathrm{d}a. \tag{6}$$

Then, $\varepsilon(r_p)$ will be given by the addition of the contributions of all impact parameters:

$$\varepsilon(r_p) = \int_0^{R_P} 2\pi a n(r_p) v_\infty(r_p) \Phi(M_r, a, r_p)\,\mathrm{d}a. \tag{7}$$

It is convenient to express ε in units of the planetesimals number density n, because n is given by the evolution of the planetary neighborhood, i.e., it is a non-local quantity. So, we define $\Psi(M_r, r_p)$ as

$$\Psi(M_r, r_p) = \frac{\varepsilon(r_p)}{n(r_p)} = 2\pi v_\infty(r_p) \int_0^{R_P} \Phi(M_r, a, r_p) a\,\mathrm{d}a. \tag{8}$$

Notice that the dependence of $\Psi(M_r, r_p)$ on the initial velocity of planetesimals $v_\infty(r_p)$ is *non* linear, since $\Phi(M_r, a, r_p)$ is also function of $v_\infty(r_p)$.

Values of Ψ corresponding to the envelopes of the set of models I considered in this paper are shown in Figs. 5–7 as a function of the radius of the envelope for the cases of $\sigma_{ab} = 10^{-1}$, 10^{-2}, and 10^{-3} s^2 km^{-2} respectively.

For the case of $\sigma_{ab} = 10^{-3}$ s^2 km^{-2} (Fig. 5), there is deposition of energy for all envelope layers. This is consequence of the fact that there are values for the impact parameter for which planetesimals move across the entire envelopes, finally impacting onto the core. For $\sigma_{ab} = 10^{-2}$ s^2 km^{-2} (Fig. 6) the situation is the same for models A to E. For the rest of the models, the only planetesimals able to reach the planetary core are the small ones. Large planetesimals are completely ablated at outer layers independently of the impact parameter (see, for example, the case of planetesimals of 100 km in panel H of Fig. 6). Finally, for the highest value of the ablation parameter, $\sigma_{ab} = 10^{-1}$ s^2 km^{-2} (Fig. 7), situation is very different because all objects are strongly ablated, so they are not able to penetrate deeply into the planetary envelope, especially for models D to H.

In Fig. 8 we show the ratio of the final to the initial energy of the planetesimals as a function of the impact parameter for the planetary envelopes corresponding to the set of models I and all planetesimal sizes. Here we assumed $\sigma_{ab} = 10^{-3}$ s^2 km^{-2}. All

[4] Notice that the integral of $\varepsilon(r_p)$ over the distribution of sizes of incoming planetesimals is one of the quantities that enter in the equation of energy conservation of planetary evolution.

Please cite this article in press as: O.G. Benvenuto, A. Brunini, The effects of ablation on the cross section of planetary envelopes at capturing planetesimals, Icarus (2008), doi:10.1016/j.icarus.2008.02.012

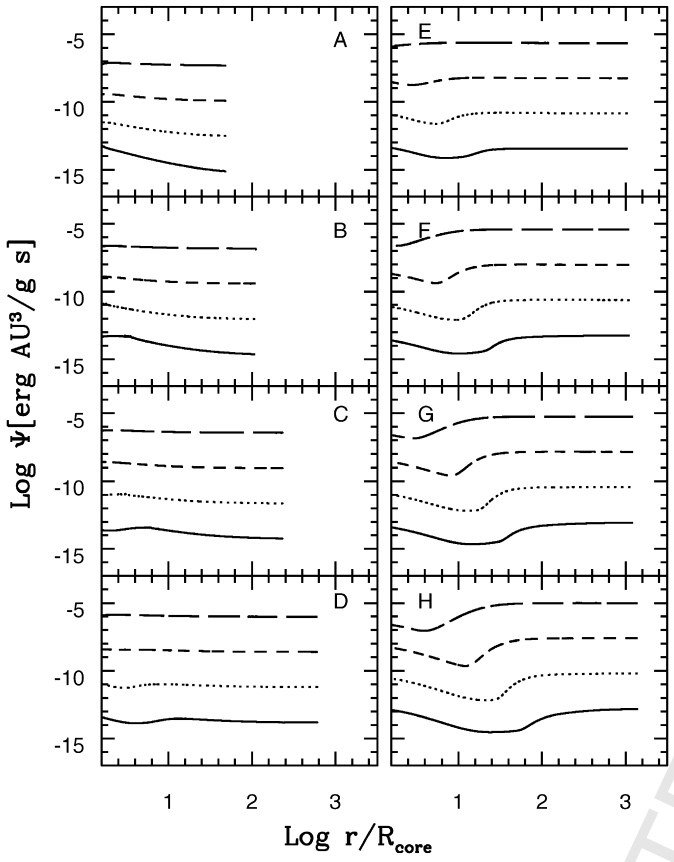

Fig. 5. The specific energy (per planetesimal number density) deposited in the planetary envelopes of the set of models I due to drag and ablation as a function of the radius inside the envelope (measured in units of the core radius). Here, solid, dot, short dash, and long dash lines represent the cases of planetesimals with radii of 0.1, 1, 10, and 100 km respectively. Here we assumed $\sigma_{ab} = 10^{-3}$ s^2 km^{-2}.

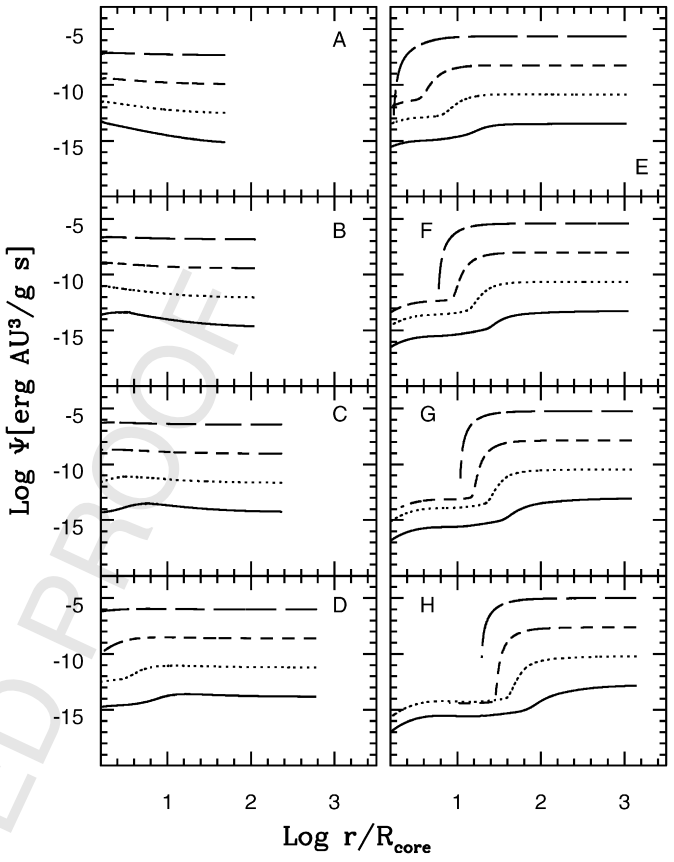

Fig. 6. Same as Fig. 5 but for the case of $\sigma_{ab} = 10^{-2}$ s^2 km^{-2}.

curves extend up to an impact parameter equal to the radius of the planet. For large impact parameters and large planetesimals, the final energy at emerging from the envelope is similar to the initial energy. As expected, the smaller the impact parameter, the lower the final energy. In the cases of the three thinner envelopes (A, B, and C), curves show minima that correspond to the case of orbits for which drag and ablation forces planetesimals to move along a nearly circular orbit along which are completely ablated. For impact parameters even smaller, some curves indicate an increase of the final energy of planetesimals. This indicates that for these values of a, planetesimals finally impact the planetary core. For the case of the rest of the model envelopes (D to H) there is no longer any minimum and below some impact parameter value, E_f is zero. This indicates that planetesimals are completely ablated and do not impact the core.

4.3. The ablated mass fraction of incoming planetesimals

In computing the mass fraction of ablated material per unit of time and per gram of the planetary envelope we shall proceed in a way similar to that employed for the case of energy deposition. This quantity should be given as a function of the planetesimal number density. We define $\Theta(M_r, a, r_p)$ as the mass deposited per gram on a layer between M_r and $M_r + \mathrm{d}M_r$ due to planetesimals of radius r_p incoming with impact parameter a. Then, we define $\Xi(M_r, r_p)$ as the mass deposited per gram, second, and planetesimal number density given by:

$$\Xi(M_r, r_p) = 2\pi v_\infty(r_p) \int_0^{R_P} \Theta(M_r, a, r_p) a \, \mathrm{d}a. \quad (9)$$

In Fig. 9 we show values of $\Xi(M_r, r_p)$ for the case of $\sigma_{ab} = 10^{-3}$ s^2 km^{-2} for the case of the set of models I. As discussed for the case of energy deposition with the same value of σ_{ab}, there is mass deposition for all envelope layers, because there are values of the impact parameter for which planetesimals move across the entire envelopes.

As we shall show below, an important quantity in computing the capturing cross section is the fractional amount of mass deposited by planetesimals that finally leave the planetary envelope: $1 - m_f/m_i$ where m_i (m_f) represents the initial (final) mass of planetesimals. In order to demonstrate the importance of this effect we show three figures, all of them corresponding to the set of models I. In the first (Fig. 10), we employed one model (D), one ablation parameter ($\sigma_{ab} = 10^{-2}$ s^2 km^{-2}) and all the planetesimal sizes. In the second (Fig. 11) we employed the same model (D), one size of planetesimals (1 km) and all the values of the ablation parameter. Finally, in Fig. 12 we employed one ablation parameter ($\sigma_{ab} = 10^{-2}$ s^2 km^{-2}), one size

Please cite this article in press as: O.G. Benvenuto, A. Brunini, The effects of ablation on the cross section of planetary envelopes at capturing planetesimals, Icarus (2008), doi:10.1016/j.icarus.2008.02.012

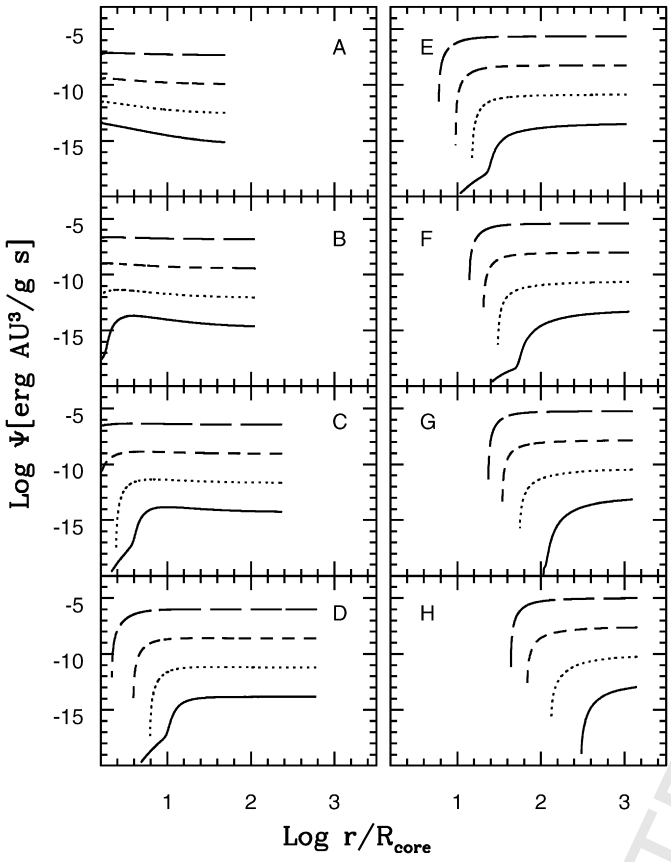

Fig. 7. Same as Fig. 5 but for the case of $\sigma_{ab} = 10^{-1}$ s^2 km^{-2}.

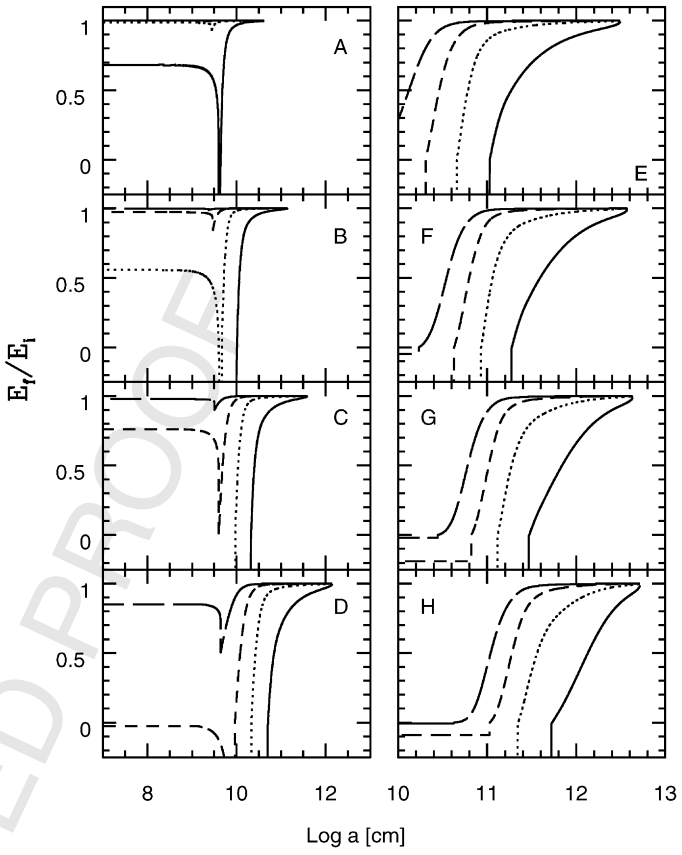

Fig. 8. The ratio of the final to the initial energy of the planetesimals as a function of the impact parameter for the case of the set of models I. As in Fig. 5, solid, dot, short dash, and long dash lines represent the cases of planetesimals with radii of 0.1, 1, 10, and 100 km, respectively. For unbounded orbits, the final energy corresponds to the moment at which the planetesimal emerges from the planet. For the rest of the cases, the final energy is computed at the moment at which the mass of the planetesimal becomes $\leqslant 10^{-6}$ of the original mass or when it reaches $r \leqslant R_{core}$. In the cases of the three thinner envelopes considered here, the minima corresponds to orbit in which the drag forces planetesimal to move along a nearly circular orbit and are completely ablated. Planetesimals incoming with a smaller impact parameter finally impact the planetary core. Here we assumed $\sigma_{ab} = 10^{-3}$ s^2 km^{-2}.

of planetesimals (1 km) and all the envelopes considered in this paper.

From these figures it can be noticed that ablation of planetesimals leaving the planet is appreciable, even for the case of impact parameters much larger than a_{crit} (in Figs. 10–12 at short radii, curves end at the corresponding a_{crit}). Thus, planets will be able to accrete an amount of mass larger than that predicted by the usually employed capture cross section πa_{crit}^2.

4.4. An estimation of the energy release due to the settling of ablated material

In this paper we shall not treat the problem of the fate of the dense material deposited in the planetary envelope due to the ablation process. Here we are interested on the dynamics of the planetesimals which leads to a local energy deposition per time unit. The energy deposition given in the present paper represents a lower limit to the total energy release due to planetesimals accretion which corresponds to the case in which dense material remains at the layers where it was ablated. If the dense deposited material migrates towards the planetary core, it will lead to a supplementary gravitational energy release per time unit, a luminosity deposition L_{dep}, that should be considered in full simulations of the growth of planetary embryos.

Notice that there will be two different timescales that determine the fate of this material: the timescales of accretion τ_a and deposition τ_d. If $\tau_a \gg \tau_d$ we have an equilibrium situation in which it can be considered that deposited material falls down quasi instantaneously, and the luminosity deposition $L_{dep}^{max}(r_p)$ due to planetesimals of radius r_p is given by

$$L_{dep}^{max}(r_p) = n(r_p) \int_{M_{core}}^{M_P} \frac{GM_r}{r} \Xi(M_r, r_p)\, dM_r. \quad (10)$$

This expression is an upper limit to the remaining luminosity deposition inside the planetary envelope. On the contrary, if $\tau_a \ll \tau_d$, the solid material will accumulate on the layers and then $L_{dep}(r_p) \approx 0$.

While usually it has been considered that accretion luminosity is released at the bottom of the envelope, the results presented here indicate that this is not the general case, especially for high values of σ_{ab}. We remark here that a proper treatment of energy deposition should be important because it is one of the ingredients that determine the structure of the whole planetary envelope and may also have non-negligible impact on the onset of the runaway growth.

Please cite this article in press as: O.G. Benvenuto, A. Brunini, The effects of ablation on the cross section of planetary envelopes at capturing planetesimals, Icarus (2008), doi:10.1016/j.icarus.2008.02.012

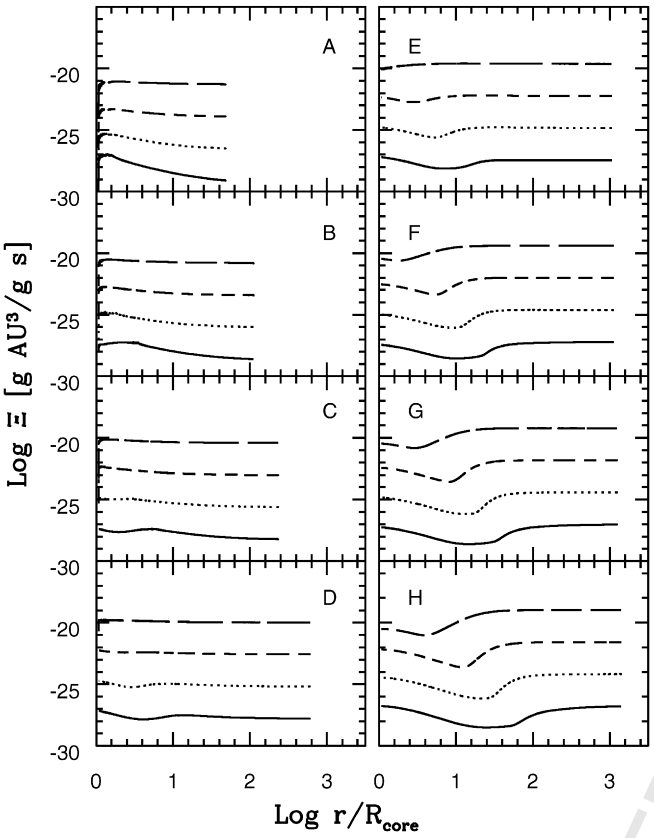

Fig. 9. The mass deposited per gram, second, and planetesimal number density given by Eq. (9) for the set of models I. Here we assumed $\sigma_{ab} = 10^{-3}$ s^2 km^{-2}. Line types are as in Fig. 5. As discussed for the case of energy deposition with the same value of σ_{ab}, there is mass deposition for all envelope layers, because there are values of the impact parameter for which planetesimals move across the entire envelopes.

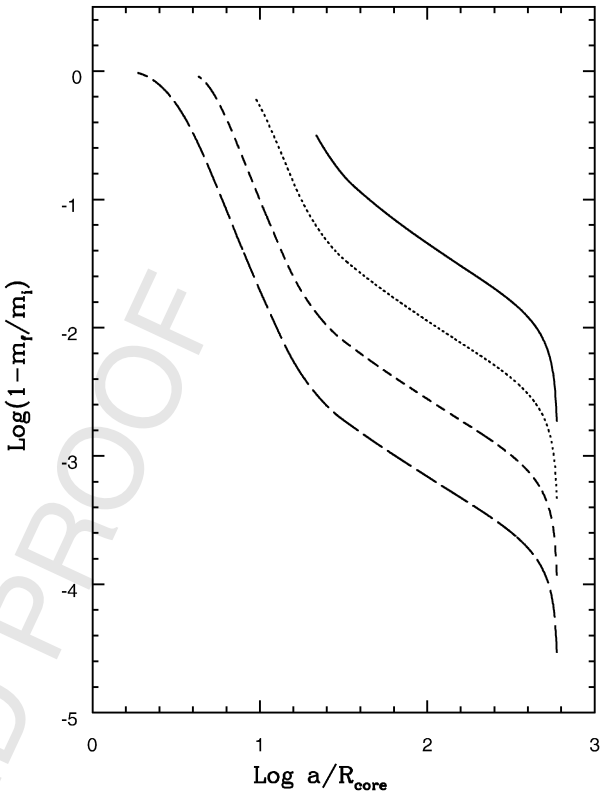

Fig. 10. The fractional amount of mass deposited by planetesimals leaving the planetary envelope D (see Table 1) as a function of the impact parameter (measured in units of the core radius). Here we assumed $\sigma_{ab} = 10^{-2}$ s^2 km^{-2}. Solid, dot, short dash, and long dash represent the cases of planetesimals with radii of 0.1, 1, 10, and 100 km, respectively. At small radii, lines extend from the a_{crit} corresponding to each planetesimal size. Notice that even for the case of $a \gg a_{crit}$ the mass deposition is non-negligible. This is relevant, because it is amplified by the Jacobian a in the integrand of Eq. (11).

It is interesting to perform an estimate of the value of the maximum available energy deposition given by Eq. (10). In Table 2, we give the corresponding values of L_{dep}^{max} for the case of $\sigma_{ab} = 10^{-3}$ s^2 km^{-2}. These values have been normalized to a luminosity of $10^{-12} L_\odot$ and a number density of one planetesimal per cubic AU. Let us consider some typical numbers, e.g., a surface density $\sigma = 10$ g cm^{-2} and a scale height for the disc of 0.2 AU. If we consider a single sized population, the planetesimal number densities will be 2×10^6, 2×10^9, 2×10^{12}, and 2×10^{15} AU^{-3} for the case of planetesimals of 100, 10, 1, and 0.1 km, respectively. With these planetesimal number densities we can evaluate L_{dep}^{max}. For the case of envelope A and planetesimals of 10 km, the maximum deposition luminosity is $L_{dep}^{max} = 6.2 \times 10^{-14} L_\odot$ while the total accretion luminosity[5] is $L_{acc} = 2 \times 10^{-8} L_\odot$. For the envelope D and the same size for planetesimals, $L_{dep}^{max} = 3.9 \times 10^{-8} L_\odot$ while $L_{acc} = 2.7 \times 10^{-5} L_\odot$. Evidently, the deposition energy is small compared to the total accretion energy available for the planet. For the case of higher values of σ_{ab}, the amount of ablated material is higher, and this will lead to a larger ratio of deposition luminosity to total accretion luminosity.

4.5. Enhanced cross sections

Because of the previous discussion it follows that, in order to compute the planetary cross section due to the capture of planetesimal material by drag and ablation we have to consider the contributions due to the three kinds of trajectories quoted above. Obviously (for a given planetesimal size) for trajectories with $a \leqslant a_{crit}$, planetesimals are completely swallowed by the planetary envelope. Now, for the case of trajectories with $a > a_{crit}$, we have shown that planetesimals undergo partial ablation. Thus, even for the case of unbound orbits, the contribution due to the material ablated from these planetesimals must be included in the evaluation of the capture cross section. The expression adopted for the total cross section of the planet is given by

$$\Sigma = \pi a_{crit}^2 + \int_{a_{crit}}^{R_P} 2\pi a \left(1 - \frac{m_f}{m_i}\right) da. \quad (11)$$

The cross section of the planetary envelopes of both sets of models considered in this paper at capturing planetesi-

[5] In computing this quantity we consider the capturing cross section described in this paper, and not the value employed in constructing the models envelopes, see Section 2.

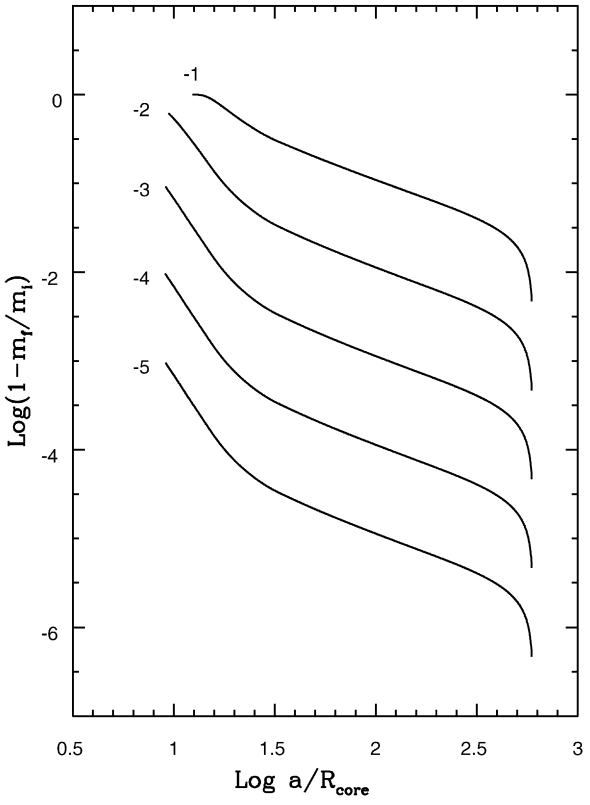

Fig. 11. The fractional amount of mass deposited by planetesimals with an initial radius of 1 km leaving the planetary envelope labeled as D (see Table 1) as a function of the impact parameter (measured in units of the core radius). Here we assumed $\log \sigma_{ab}$ [$s^2\,km^{-2}$] = −1, −2, −3, −4, and −5. Curves are labeled with the corresponding $\log \sigma_{ab}$ values.

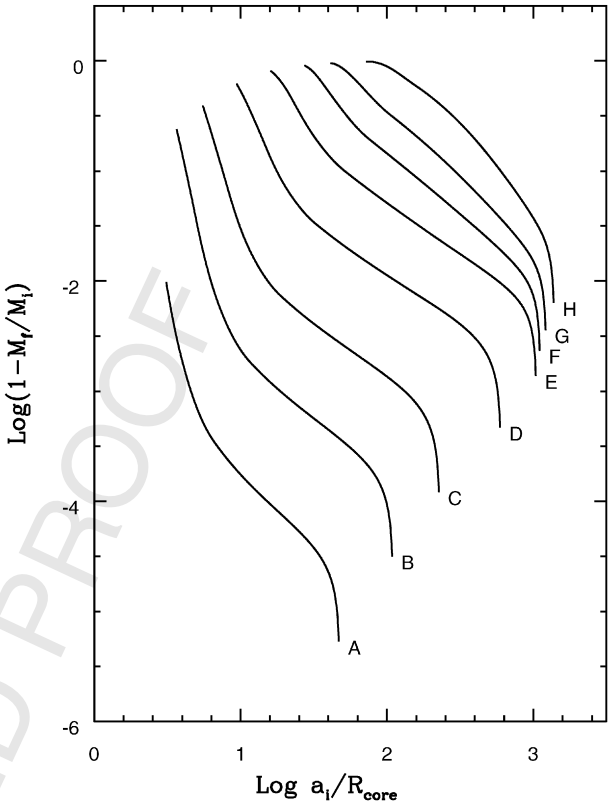

Fig. 12. The fractional amount of mass deposited by planetesimals with an initial radius of 1 km leaving the planetary envelopes considered in this paper (see Table 1) as a function of the impact parameter (measured in units of the core radius). Here we assumed $\sigma_{ab} = 10^{-2}\ s^2\,km^{-2}$. As expected, the fraction of mass ablated during the passage across the planetary envelopes is a steeply increasing function upon the mass of the envelope.

mals of 0.1, 1, 10, and 100 km for the cases of $\log \sigma_{ab} = -1, -2, -3, -4$, and -5 are given in Tables 3–7, respectively, and depicted in Figs. 13–14. These results indicate that the ablation parameter σ_{ab} is important for determining the capture cross sections of planetesimals.

Let us define the enhancement of the cross sections Γ due to the ablated material to emerging planetesimals as

$$\Gamma \equiv \frac{\Sigma}{\pi a_{crit}^2}. \tag{12}$$

Values of Γ for the set of models and sizes of planetesimals are presented in Fig. 15. For the case of tiny gaseous envelopes as those corresponding to models A and B, Γ is important only for high values of σ_{ab}. However, for the case of model C, with an envelope of only $0.0245 M_\oplus$, Γ is large for high σ_{ab} values but it is also non-negligible for lower values of the ablation parameter. For the rest of the planetary envelope models considered in this paper, Γ is large. Notably, for some of the explored cases, Γ has a non-monotonous dependence neither upon the size of incoming planetesimals nor with σ_{ab}. In any case it should be remarked that for all the model envelopes and sizes of planetesimals considered in this paper, the case of $\log \sigma_{ab} = -5$ gives results very similar to those we would have found neglecting ablation.

5. Discussion and conclusions

In this paper we have studied the effects of drag and ablation on the cross section of planetary envelopes for the capture of planetesimals. In doing so we have employed two sets of eight planetary envelope models computed with a detailed giant planet growth code assuming the oligarchic growth regime for the accretion of material onto the core. These sets of models were selected in order to represent all the stages of planetary formation. In order to account for the uncertainties in the models, the set of models I and II were computed assuming a nebula with 10 and 5 times the mass corresponding to the minimum mass solar nebula, respectively. The trajectories of planetesimals were computed neglecting the gravitation of the central star of the system. We considered planetesimals with radii from 0.1 to 100 km and values for the ablation coefficient from 10^{-1} to $10^{-5}\ s^2\,km^{-2}$. The velocities of the planetesimals at entering the planetary envelope have been computed by assuming the oligarchic growth regime (Ida and Makino, 1993), which are higher than those computed with the prescriptions given in Greenzweig and Lissauer (1990, 1992). We should remark that because the velocity regime and the core accretion were computed in the same regime, this makes our calculation self consistent in this important aspect.

Please cite this article in press as: O.G. Benvenuto, A. Brunini, The effects of ablation on the cross section of planetary envelopes at capturing planetesimals, Icarus (2008), doi:10.1016/j.icarus.2008.02.012

Table 2
Logarithm of the maximum deposition luminosity $L_{\rm dep}^{\rm max}(r_p)$ given by Eq. (10) for the case of $\sigma_{\rm ab} = 10^{-3}$ s^2 km^{-2} and different sizes of planetesimals

Model	$r_p = 0.1$ km	$r_p = 1$ km	$r_p = 10$ km	$r_p = 100$ km
A	−14.35	−12.59	−10.50	−8.230
B	−12.40	−9.984	−7.876	−5.610
C	−11.19	−8.630	−6.149	−3.837
D	−9.833	−7.325	−4.708	−2.157
E	−8.757	−6.278	−3.664	−0.922
F	−8.054	−5.550	−2.925	−0.137
G	−7.555	−5.079	−2.462	0.334
H	−6.929	−4.517	−1.928	0.886

Values are given in units of $10^{-12} L_\odot$ and normalized for a planetesimal number density $n = 1$ AU^3.

Table 3
Logarithm of the total cross section (in units of cm^2), for the four sizes of planetesimals considered in this paper (given in parentheses), of the planetary envelope models included in Table 1

Model	log Σ [cm^2]			
	$r_p = 0.1$ km	$r_p = 1$ km	$r_p = 10$ km	$r_p = 100$ km
A	19.91	19.42	19.12	18.92
B	21.07	20.46	19.90	19.47
C	22.34	21.74	21.16	20.59
D	23.92	23.35	22.77	22.18
E	24.96	24.44	23.87	23.29
F	25.31	24.86	24.32	23.75
G	25.56	25.18	24.68	24.14
H	25.83	25.56	25.15	24.65
A*	19.54	19.02	18.70	18.48
B*	20.21	19.59	19.10	18.78
C*	21.11	20.52	20.01	19.57
D*	22.25	21.67	21.12	20.64
E*	23.11	22.54	21.98	21.46
F*	23.96	23.41	22.85	22.30
G*	24.96	24.45	23.91	23.36
H*	25.71	25.37	24.91	24.41

These results correspond to the case of $\sigma_{\rm ab} = 10^{-1}$ s^2 km^{-2}.

Table 4
Same as Table 3 but for the case of $\sigma_{\rm ab} = 10^{-2}$ s^2 km^{-2}

Model	log Σ [cm^2]			
	$r_p = 0.1$ km	$r_p = 1$ km	$r_p = 10$ km	$r_p = 100$ km
A	19.77	19.36	19.10	18.91
B	20.61	19.96	19.51	19.27
C	21.55	20.92	20.33	19.84
D	22.99	22.40	21.81	21.24
E	24.06	23.49	22.90	22.33
F	24.49	23.94	23.38	22.84
G	24.83	24.32	23.78	23.24
H	25.26	24.82	24.30	23.78
A*	19.46	18.99	18.69	18.48
B*	20.03	19.40	18.96	18.73
C*	20.72	20.12	19.60	19.16
D*	21.54	20.96	20.47	20.02
E*	22.27	21.70	21.19	20.75
F*	23.07	22.50	21.97	21.50
G*	24.09	23.55	23.01	22.53
H*	25.05	24.58	24.08	23.61

Table 5
Same as Table 3 but for the case of $\sigma_{\rm ab} = 10^{-3}$ s^2 km^{-2}

Model	log Σ [cm^2]			
	$r_p = 0.1$ km	$r_p = 1$ km	$r_p = 10$ km	$r_p = 100$ km
A	19.75	19.36	19.10	18.91
B	20.50	19.84	19.44	19.25
C	21.20	20.52	19.83	19.55
D	22.23	21.58	20.96	20.37
E	23.17	22.57	21.98	21.39
F	23.62	23.05	22.49	21.97
G	23.99	23.43	22.90	22.41
H	24.46	23.95	23.44	22.96
A*	19.45	18.99	18.69	18.48
B*	20.01	19.37	18.95	18.73
C*	20.65	20.04	19.46	19.04
D*	21.29	20.70	20.15	19.52
E*	21.82	21.22	20.71	20.17
F*	22.46	21.82	21.33	20.87
G*	23.32	22.74	22.26	21.85
H*	24.26	23.76	23.31	22.92

Table 6
Same as Table 3 but for the case of $\sigma_{\rm ab} = 10^{-4}$ s^2 km^{-2}

Model	log Σ [cm^2]			
	$r_p = 0.1$ km	$r_p = 1$ km	$r_p = 10$ km	$r_p = 100$ km
A	19.75	19.36	19.10	18.91
B	20.49	19.83	19.43	19.24
C	21.14	20.45	19.71	19.51
D	21.95	21.22	20.50	19.89
E	22.66	21.97	21.31	20.54
F	23.14	22.49	21.90	21.21
G	23.52	22.87	22.28	21.64
H	24.01	23.34	22.75	22.12
A*	19.45	18.99	18.69	18.48
B*	20.00	19.37	18.95	18.73
C*	20.64	20.03	19.44	19.03
D*	21.26	20.66	20.09	19.35
E*	21.73	21.12	20.60	19.92
F*	22.30	21.60	21.13	20.55
G*	23.02	22.38	21.92	21.37
H*	23.87	23.29	22.80	22.20

We find that the high velocities prescribed by the oligarchic growth regime for incoming planetesimals (see Fig. 1), have deep consequences for the calculation of planetary cross section. This is so for both sets of models considered in this paper. Notice that the rate of ablation depends on the velocity to the third power. Then, it is not surprising that while in previous works (Inaba and Ikoma, 2003) ablation has been considered as negligible at computing cross sections, here we found it important.

We have performed some calculations in order to compare our results with those of Inaba and Ikoma (2003) in which we have assumed velocities of the incoming planetesimals given by $r_H \Omega_K M_p / M_\oplus$ (where r_H is the corresponding Hill's radius and Ω_K is the Keplerian angular velocity) as in Inaba and Ikoma (2003). For the case of the small cores explored by these authors, our results indicate that, indeed, ablation has negligible impact on the capture cross section in agreement with the

Table 7
Same as Table 3 but for the case of $\sigma_{ab} = 10^{-5}$ s^2 km^{-2}

Model	log Σ [cm^2]			
	$r_p = 0.1$ km	$r_p = 1$ km	$r_p = 10$ km	$r_p = 100$ km
A	19.75	19.36	19.10	18.91
B	20.49	19.83	19.43	19.24
C	21.14	20.44	19.70	19.50
D	21.90	21.16	20.42	19.79
E	22.55	21.82	21.12	20.11
F	23.04	22.36	21.74	20.88
G	23.42	22.73	22.12	21.26
H	23.92	23.18	22.51	21.55
A*	19.45	18.99	18.69	18.48
B*	20.00	19.37	18.95	18.73
C*	20.64	20.03	19.44	19.03
D*	21.25	20.65	20.09	19.33
E*	21.72	21.11	20.58	19.89
F*	22.28	21.57	21.10	20.50
G*	22.97	22.31	21.86	21.25
H*	23.80	23.20	22.68	21.79

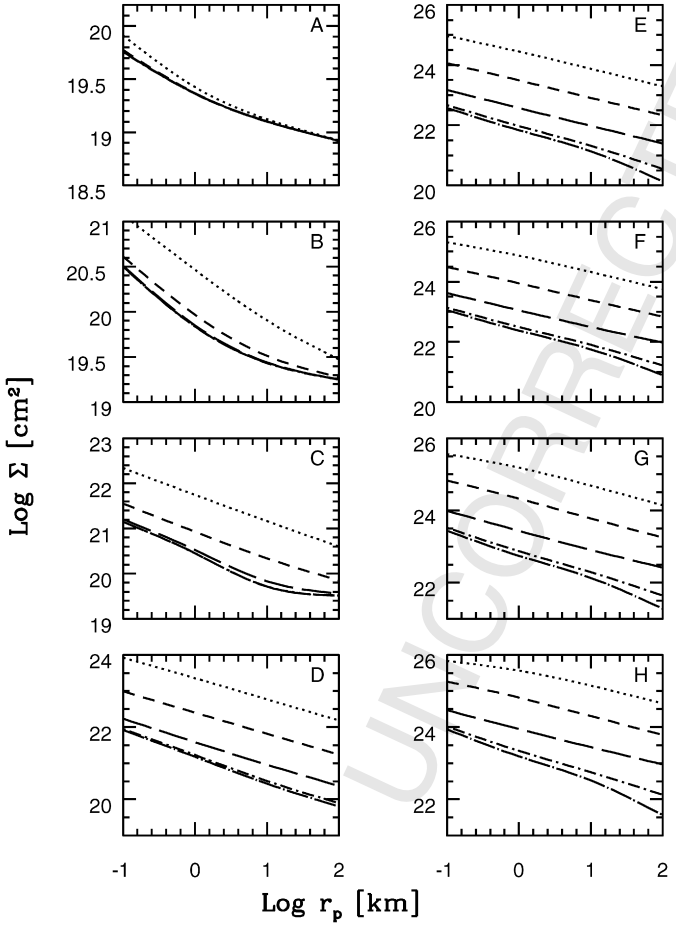

Fig. 13. The cross section of planetary envelopes corresponding to the eight models of set I as a function of the planetesimal. Here dot lines, short dash, long dash, dot–short dash and dot–long dash lines represent the cases for which $\sigma_{ab} = 10^{-1}$, 10^{-2}, 10^{-3}, 10^{-4}, and 10^{-5} s^2 km^{-2}, respectively. The case of $\sigma_{ab} = 10^{-5}$ s^2 km^{-2} gives results very similar to those we would have found by neglecting ablation. Notice that the cross section of planetary envelopes is steeply dependent on the value of σ_{ab}, especially for the case of thick envelopes.

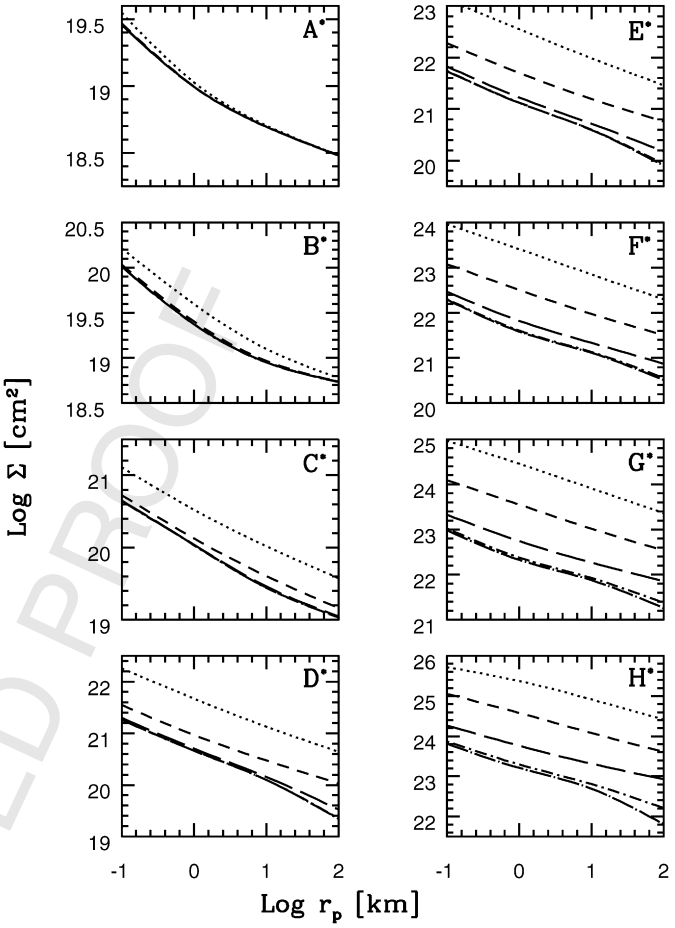

Fig. 14. Same as Fig. 13 but for the case of the set of models II.

results of the referred paper. However, even for these low velocity values, ablation is important in determining the capture cross section of planets with cores larger than those considered by Inaba and Ikoma (2003). Because of this reason, our results are fairly complimentary to those presented in the above referred paper.

The increase of the cross section due to ablation presented in this paper is significant and should accelerate the growth of planetary embryos compared to models that ignore such an effect. Also, the results presented above indicate that, in computing accurate capture cross sections the effects due to ablation are so relevant that justify the inclusion, in future calculations, of a more detailed treatment of ablation than the one adopted in this paper.

In the frame of the oligarchic growth scenario, capture cross sections including ablation represents an important ingredient to be considered in the next generation of models of planetary formation that should include a distribution of sizes for the incoming planetesimals. Doing so will allow us to construct planetary formation models far more detailed than the present ones. This, in turn will allow to reexamine the difficulties related to the timescale of planetary growth as compared to the timescales of dissipation of protoplanetary nebulae in the reference frame of more plausible models.

Please cite this article in press as: O.G. Benvenuto, A. Brunini, The effects of ablation on the cross section of planetary envelopes at capturing planetesimals, Icarus (2008), doi:10.1016/j.icarus.2008.02.012

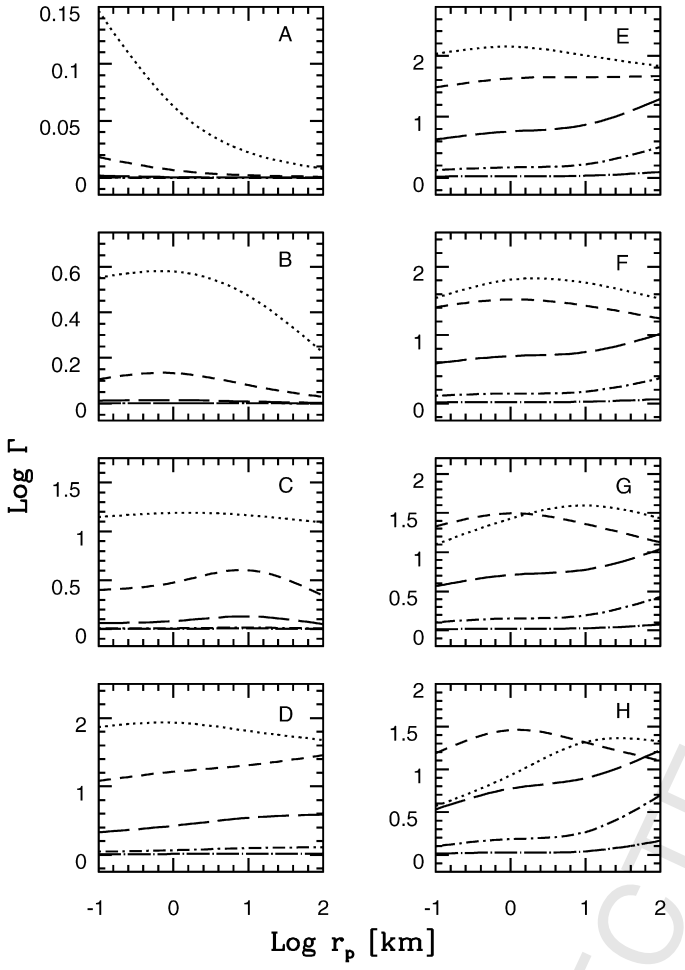

Fig. 15. The enhancement Γ of the cross section of planetary envelopes due to the ablation of planetesimals on open orbits as a function of the planetesimal radii for the eight planetary envelopes considered in this paper. The meaning of labels and lines is the same as in Fig. 13. While for the thinner envelopes the enhancement is noticeable only for high values of σ_{ab}, the effect becomes also very large for the case of more massive envelopes and lower values of σ_{ab}.

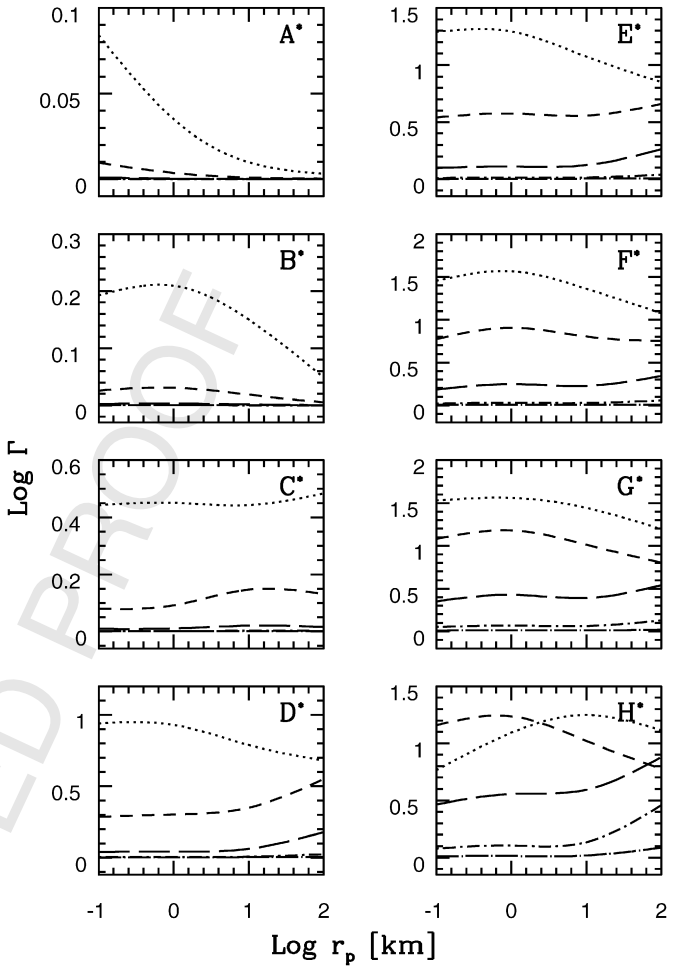

Fig. 16. Same as Fig. 15 but for the case of the set of models II.

References

Alibert, Y., Mordasini, C., Benz, W., Winisdoerffer, C., 2005. Models of giant planet formation with migration and disc evolution. Astron. Astrophys. 434, 343–353.

Benvenuto, O.G., Brunini, A., 2005. Methods for computing giant planet formation and evolution. Mon. Not. R. Astron. Soc. 356, 1383–1395.

Bodenheimer, P., Pollack, J.B., 1986. Calculations of the accretion and evolution of giant planets: The effects of solid cores. Icarus 67, 391–408.

Brunini, A., Melita, M.D., 2002. On the accretion of Uranus and Neptune. Mon. Not. R. Astron. Soc. 330, 184–186.

Chambers, J., 2006. A semi-analytic model for oligarchic growth. Icarus 180, 496–513.

Fortier, A., Benvenuto, O.G., Brunini, A., 2007. Oligarchic planetesimal accretion and giant planet formation. Astron. Astrophys. 473, 311–322.

Greenberg, R., Hartmann, W.K., Chapman, C.R., Wacker, J.F., 1978. Planetesimals to planets—Numerical simulation of collisional evolution. Icarus 35, 1–26.

Greenzweig, Y., Lissauer, J.J., 1990. Accretion rates of protoplanets. Icarus 87, 40–77.

Greenzweig, Y., Lissauer, J.J., 1992. Accretion rates of protoplanets. II. Gaussian distributions of planetesimal velocities. Icarus 100, 440–463.

Guillot, T., 2005. The interiors of giant planets: Models and outstanding questions. Annu. Rev. Earth Planet. Sci. 33, 493–530.

Hayashi, C., 1981. Structure of the solar nebula, growth and decay of magnetic fields and effects of magnetic and turbulent viscosities on the nebula. Prog. Theor. Phys. Suppl. 70, 35–53.

Hollenbach, D.J., Yorke, H.W., Johnstone, D., 2000. Disk dispersal around young stars. Protostars Planets IV, 401.

Ida, S., Makino, J., 1993. Scattering of planetesimals by a protoplanet—Slowing down of runaway growth. Icarus 106, 210.

Ikoma, M., Nakazawa, K., Emori, H., 2000. Formation of giant planets: Dependences on core accretion rate and grain opacity. Astrophys. J. 537, 1013–1025.

Inaba, S., Ikoma, M., 2003. Enhanced collisional growth of a protoplanet that has an atmosphere. Astron. Astrophys. 410, 711–723.

Inaba, S., Wetherill, G.W., Ikoma, M., 2003. Formation of gas giant planets: Core accretion models with fragmentation and planetary envelope. Icarus 166, 46–62.

Kokubo, E., Ida, S., 1996. On runaway growth of planetesimals. Icarus 123, 180–191.

Kokubo, E., Ida, S., 1998. Oligarchic growth of protoplanets. Icarus 131, 171–178.

Mizuno, H., 1980. Formation of the giant planets. Prog. Theor. Phys. 64, 544–557.

Please cite this article in press as: O.G. Benvenuto, A. Brunini, The effects of ablation on the cross section of planetary envelopes at capturing planetesimals, Icarus (2008), doi:10.1016/j.icarus.2008.02.012

Podolak, M., Pollack, J.B., Reynolds, R.T., 1988. Interactions of planetesimals with protoplanetary atmospheres. Icarus 73, 163–179.

Pollack, J.B., Hubickyj, O., Bodenheimer, P., Lissauer, J.J., Podolak, M., Greenzweig, Y., 1996. Formation of the giant planets by concurrent accretion of solids and gas. Icarus 124, 62–85.

Press, W.H., Teukolsky, S.A., Vetterling, W.T., Flannery, B.P., 1992. Numerical recipes in FORTRAN: The Art of Scientific Computing. Cambridge Univ. Press, Cambridge.

Thommes, E.W., Duncan, M.J., Levison, H.F., 2003. Oligarchic growth of giant planets. Icarus 161, 431–455.

Please cite this article in press as: O.G. Benvenuto, A. Brunini, The effects of ablation on the cross section of planetary envelopes at capturing planetesimals, Icarus (2008), doi:10.1016/j.icarus.2008.02.012